Development and Preliminary Evaluation of a MRI-guided Transrectal Prostate Intervention

A. Krieger[1,2], S. Song[3], N. B. Cho[3], P. Guion[4], I. Iordachita[1], G. Fichtinger[5], and L. L. Whitcomb[1]

[1]Department of Mechanical Engineering, The Johns Hopkins University, Baltimore, MD, United States, [2]Sentinelle Medical Inc., Toronto, Canada, [3]Engineering Research Center, The Johns Hopkins University, Baltimore, MD, United States, [4]National Institute of Health, Bethesda, MD, United States, [5]School of Computing, Queen's University, Kingston, Ontario, Canada

Introduction

Numerous studies have shown that transrectal ultrasound (TRUS) - guided prostate biopsy fails to detect cancer in significant numbers, since contemporary ultrasound cannot resolve target lesions [1]. Improved biopsy targeting with magnetic resonance imaging (MRI) could potentially overcome the shortcomings of ultrasound for the diagnosis and local therapy for prostate cancer. To utilize such advantages, a number of MRI-compatible prostate intervention systems were introduced. However, previously reported systems require the patient to be removed from the MRI scanner during the interventional procedure. A fully actuated robot, however, enables both imaging and interventional procedures to be performed entirely inside the scanner without removing the patient. Moreover, a fully actuated robot could simplify and speed up the procedure; allow for real-time needle insertion visualization; enable detection of prostate deformation, misalignment, and deflection of the needle; and allow for on-the-spot corrections to needle placements.

Materials and Methods

Fig. 1 (a) shows a CAD model of the automated prostate robot. The robot employs similar or identical manipulator mechanism to the APT-MRI system reported in [2]. The robot consists of a rotation stage and a translation stage with flexible coupling, integrated in a motor box. Non-magnetic piezo-ceramic motors (HR series, Nanomotion Inc.) were used for actuation. The robot is constructed mostly of plastic materials, fore-most of Ultem, selected for its structural stability and machinability. The robot uses the hybrid tacking method described in [1]. Robot registration is performed using four Beekley markers (Beekley Inc.) integrated into the rectal sheath and the needle channel. The initial position and orientation of the robot is computed after automatic segmentation of the markers on MRI images. Modular EMI electro-optical encoders (US Digital), code wheel, and code strip were selected for joint encoding. The controller box contains two Nanomotion AB5 motor amplifiers, a DMC-21x3 Ethernet motion controller (Galil Motion Control), and a EIR-M-ST fiber optic to Ethernet media converter (B&B Electronics Mfg. Co.). The only electrical connection to the controller is a filtered 24V DC power supply through the scanner room penetration panel. External communication is via fiber optic Ethernet.

In order to determine the effects of the robot on signal-to-noise-ratio (SNR) of the MRI images, a MRI compatibility study was conducted based on National Electrical Manufacturers Association (NEMA) standard method [3]. Tests were performed on a 3T Philips Archieva scanner (Philips Medical Systems). Three imaging sequences using the same imaging parameters were used for the compatibility study of the robot: Tl, T2 and TFE. Each set of experiments consisted of the phantom being imaged alone (baseline) and subsequently imaged under following eleven configurations: 1) Baseline. 2) Off-US: Image the phantom after placing the robot. The phantom and sheath position approximate prostate and sheath position in a clinical procedure. The controller is located in the scanner room but is powered off. 3) Off-SH: As per (2), with additional shielding. 4) Disabled-US: Image the phantom after powering the controller on but disabling the motor amplifiers. 5) Disabled-SH: As per (4), with additional shielding. 6) Roll-US: Image the phantom with the roll motor amplifier enabled, but the motor not moving. 7) Roll-SH: As per (6), with additional shielding. 8) Pitch-US: Image the phantom with the pitch motor amplifier enabled. 9) Pitch-SH: As per (8), with additional shielding. 10) Both-US: Image the phantom with both roll and pitch motor amplifiers enabled. 11) Both-SH: As per (10), with additional shielding. In configurations 3, 5, 7, 9, and 11 the system was covered with additional radio-frequency (RF) shielding (Z-3250-CN High Performance EMI Shielding Cloth, Zippertubing Co.). Ten image slices were obtained of the phantom for each configuration for each image sequence. Fig. 1 (b) shows the SNR test setup.

Results and Conclusion

The most significant observations of the MRI compatibility study are: 1) The SNR exhibits modest spatial variation - measurements were uniform across the multiple slices of a single scan sequence. 2) The robot does not cause any reduction in SNR in the motors-off configuration - thus enabling interleaved imaging and motion. 3) Turning the controller on with motors disabled reduces the SNR by 50% in without RF shielding, but SNR is only slightly degraded with RF shielding. 4) Turning the controller on with motors enabled reduces the SNR by 80% without RF shielding, but SNR is only reduced by 40% to 60% with RF shielding. 5) Noise appears as vertical 'zipper' streaks in the MR images - a well-known effect of RF interference. 6) All three sequences show similar SNR behavior. 7) The addition of RF shielding improves the SNR by a factor 200% to 500% in comparison to the same robot without RF shielding. Fig. 1 (c) illustrates the SNR results.

This study reported the design and preliminary MRI compatibility evaluation of an actuated transrectal prostate robot for MRI-guided intervention. The current version of the robot employs actuated needle guide positioning and manual needle insertion. Piezo-ceramic motors were selected as actuators for the robot. The addition of RF shielding significantly improved image SNR quality. In a study of seven MRI-guided biopsy needle placements in a prostate phantom, average in-plane error for the biopsy needles was 2.4 mm with a maximum error of 3.7 mm [4].

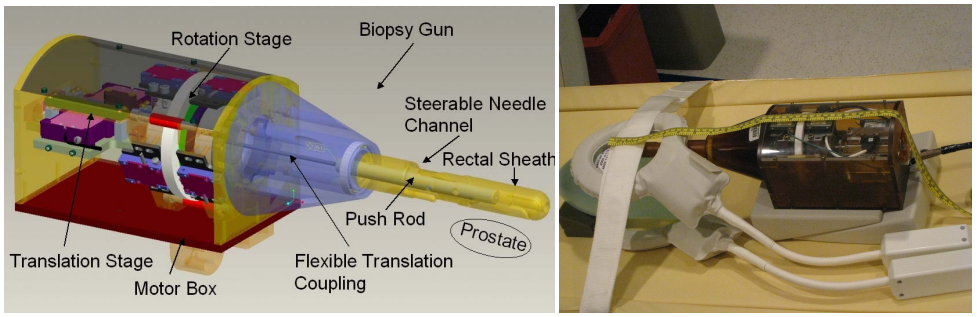

Fig. 1: (a) CAD model of the Transrectal Prostate Intervention, (b) the robot in SNR test setup, and (c) SNR results, averaged for the 10 slices, for the three sequences.

References

[1] M. Norberg, L. Egevad, L. Holmberg, P. Sparn, B. J. Norln, and C. Busch. The sextant protocol for ultrasound-guided core biopsies of the prostate underestimates the presence of cancer. *Urology*. 50(4):562-566, Oct 1997.

[2] A. Krieger, G. Metzger, G. Fichtinger, E. Atalar, and L. L. Whitcomb. A hybrid method for 6-DOF tracking of MRI-compatible robotic interventional devices. In *Proceedings - IEEE International Conference on Robotics and Automation,* volume 2006, pages 3844-3849, Orlando, FL, United States, May 2006.

[3] *Determination of Signal-to-Noise Ratio (SNR) in Diagnostic Magnetic Resonance Imaging, NEMA Standard Publication MS 1-2008.* The Association of Electrical and Medical Imaging Equipment Manufacturers, 2008.

[4] A. Krieger. *Advances in Magnetic Resonance Image Guided Robotic Intervention*. PhD thesis, Johns Hopkins University, 2008.